# The Effect of Protonation Site on Bond Strengths in Simple Peptides: Application of Ab Initio and Modified Neglect of Differential Overlap Bond Orders and Modified Neglect of Differential Overlap Energy Partitioning

Árpád Somogyi* and Vicki H. Wysocki
Department of Chemistry, Virginia Commonwealth University, Richmond, Virginia, USA

István Mayer
Central Research Institute for Chemistry of the Hungarian Academy of Sciences, P. O. Box 17, H-1525 Budapest, Hungary

A comparative study of ab initio 6-31G* and semiempirical modified neglect of differential overlap (MNDO) bond orders and MNDO diatomic energy contributions for the description of bond strengths in neutral and protonated glycine, diglycine, triglycine, and dialanine is presented. Good correlations were found between 6-31G* and MNDO bond orders and between MNDO bond orders and diatomic energy contributions. Although bond orders and diatomic energy contributions are inherently different quantities, both predict the changes in bond strengths due to protonation to be qualitatively the same. The theoretically predicted differences in bond strengths for different protonated forms clearly indicate that in peptide fragmentation schemes one should consider even those protonated forms whose formation is not preferred energetically. *(J Am Soc Mass Spectrom 1994, 5, 704–717)*

The investigation of protonated peptides by tandem mass spectrometry is of increasing importance. The fragmentation pattern allows determination of the sequence of a given peptide, which provides an alternative to "classical" sequence analysis. Although useful and important mechanisms for peptide fragmentation have been suggested [1–12], several questions still remain. For example, the role of protonation is not understood in detail due to both experimental and theoretical limitations. Experimentally, the proton affinities (PA) can be measured with acceptable accuracy (see, however, the problems associated with inappropriate application of the kinetic method [13] and recent works on "fixing" the PA scale [14]). However, the position of the proton in amino acids or oligopeptides cannot be located unambiguously. Recent work by Fenselau and co-workers [15] is a good example of this. As they noted, their work provided "experimental support for the existence of intramolecular hydrogen bonding in $Gly_3$ and $Gly_4$. However, the possible structures (conformations) of the protonated peptides are probably large in number" [15] and only an intuitively assumed conformation was presented.

In principle, the geometry and electronic structure of all of the possible protonated forms of a molecule (including intramolecular H-bond structures) can be calculated with reliable accuracy by using quantum chemical methods. This is a significant advantage, because we are not restricted by any assumptions regarding the protonation site, that is, we can probe all possible forms, even those whose formation is less preferred energetically. Unfortunately, in practice, the application of higher level ab initio calculations (especially beyond the Hartree–Fock level) is limited by the size of the molecules. In this respect, even a dipeptide can be too large, especially if one residue has a long side chain such as that of arginine or lysine. In spite of the increasing number of articles reporting ab initio calculations on amino acid [16a] and oligopeptide conformations [16b, c] and protonation of simple amino acids [17, 18] or diglycine [18], at present, we must still rely on (1) simplified models and (2) lower levels of calculations, for example, semiempirical methods [modified neglect of differential overlap (MNDO) [19a], MNDO, parametric method 3 (MNDO-PM3) [19b], Austin model 1 (AM1) [19c], etc.].

Address reprint requests to Dr. Árpád Somogyi, Department of Chemistry, Virginia Commonwealth University, Richmond, VA 23284-2006.
*On leave from Central Research Institute for Chemistry of the Hungarian Academy of Sciences, P.O. Box 17, H-1525 Budapest, Hungary.


1044-0305/94/$7.00

Received December 6, 1993
Revised March 2, 1994
Accepted March 6, 1994

Every mass spectral fragmentation is obviously a dynamic process, during which some bonds are being cleaved [and other bond(s) may be formed, i.e., in rearrangement processes]. In the great majority of cases, the detailed "dynamic" description of the fragmentation process, or even the determination of the fine details of the potential surface, is practically impossible. Instead, a "simplified" energetic treatment quite often is applied that is based on calculating energetic and thermodynamic properties of the fragmenting ions and fragments that appear in a given fragmentation process; calculations for transition states also often are made. An excellent recent overview by Radom [20] gives further details on the energetic calculations. Unfortunately, the semiempirical methods (MNDO, PM3, AM1) provide less accurate energetic data. For example, these methods are often regarded to be inaccurate for the description of peptide conformations [17a].

In spite of the difficulties sketched above, detailed descriptions of the potential energy surfaces are not always necessary to interpret mass spectral fragmentation. There is no reason to distrust the empirical rules of mass spectral fragmentation, including those for peptide fragmentation, that were established through experiments. The fact that these rules work extremely well in mass spectrometry clearly indicates that there are some simple underlying physical factors that influence fragmentation [21], and are determined by the structure of the parent molecule and its molecular ion. Therefore, it may be assumed that there should be important links between "static" parameters (derivable, e.g., from quantum mechanical wave functions) and "dynamic" fragmentation processes [22, 23]. In this article, we use two different static parameters—bond orders and diatomic energy contributions—to predict bond strengthening and bond weakening in protonated peptides. As will be shown, these quantities may lead to improved understanding and better predictions of peptide fragmentation processes.

Bond orders, valencies, and free valencies calculated from MNDO and ab initio wave functions can provide a useful basis for the description of ion structures and primary fragmentation processes [23–33]. Comparative studies [29, 30] also showed that for species containing hydrogen and first row elements, the semiempirical MNDO bond orders are in good agreement with those calculated from STO-3G, 6-31G**, and double zeta with polarization functions (DZP) self-consistent field (SCF) ab initio wave functions according to the scheme [34–36] sometimes called [37] Mulliken–Mayer population analysis (MMA). Note that in the neglect of differential overlap (NDO, such as MNDO) approximations, the MMA bond orders are the previously defined Wiberg [38] indexes. In a recent article, we successfully applied MNDO bond orders for the description of peptide fragmentation [33]. One of the main conclusions of that article is that different protonation sites (i.e., amide oxygen, amide nitrogen, terminal amino, and terminal carboxyl group) have significantly different effects on bond strengthening or bond weakening of the neighboring chemical bonds. For example, protonation on the amide oxygen leads to significant strengthening of the amide bond, that is, it makes the bond more difficult to cleave. On the other hand, protonation on the amide nitrogen (which is less favored energetically than the protonation on the amide oxygen) leads to significant weakening of the amide bond. Cleavage of the weakened amide bond (in the amide nitrogen protonated form) leads to a **b** ion, which can then fragment by CO loss to form an **a** ion. (Throughout this article we use the modified form [1] of the Roepstorff and Fohlman [39] nomenclature for the denotation of peptide fragment ions; see Scheme I.)

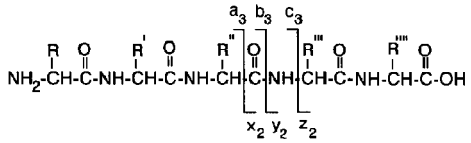


**Scheme I**

Note at this point that bond orders are not the only quantities that can be used to discuss bond strengths. Bond order and Wiberg indexes reflect the actual multiplicity of the bonds in question; they are related to bond strengths but they are not energetic quantities that can be related directly to the energy consumption of the bond cleavage processes [21]. To relate the changes in bond strengths to the energy scale, Mayer and Gömöry [21, 22] recently suggested use of the energy partitioning method, the results of which are expressed as energy.

It is well known that the total restricted Hartree–Fock (RHF) energy of a closed-shell species (such as a protonated peptide) or that of an ion treated by the "half-electron" scheme can be written as

$$E = \sum_{\mu,\nu} h_{\mu\nu} D_{\mu\nu} + \frac{1}{2} \sum_{\mu,\nu,\rho,\tau} \left( D_{\rho\mu} D_{\tau\nu} - \frac{1}{2} D_{\rho\nu} D_{\tau\mu} \right) (\mu\rho|\nu\tau) + \sum_{A<B} (Z_A Z_B / R_{AB})$$

[Here, we use the usual notation for the elements of the one electron matrix **h**, density matrix **D**, two electron integrals in the (11|22) convention, as well as nuclear charges $Z_A$ and internuclear distances $R_{AB}$.] Because there are only one- and two-center integrals in the MNDO scheme, the MNDO total energy can be presented unambiguously as a sum of intra-atomic and diatomic contributions, similarly to other semiempirical theories [40]. The actual scheme used is based on the energy presented as

$$E = \frac{1}{2} \mathrm{tr}[(\mathbf{h} + \mathbf{F})\mathbf{D}] + \sum_{A<B} (Z_A Z_B / R_{AB})$$

where **F** is the usual Fock matrix. Off-diagonal elements $h_{\mu\nu}$ and $F_{\mu\nu}$ with orbital indexes $\mu$ and $\nu$ that correspond to different atoms should be multiplied simply by $1/2\ D\nu\mu$ and added to the respective two-center contribution. Of course, the latter also should include the repulsion between the relevant nuclei. With regard to the diagonal elements of matrices **h** and **F**, those components that represent true one-center terms and those that originate from the Coulombic interaction with the nuclei and electrons of other atoms should be calculated separately and assigned to the one-center and two-center energy components, respectively [21, 22].

The diatomic energy contribution that corresponds to a given pair of atoms thus represents a quantity that conceptually differs from the bond order. It is an energetic quantity (expressed here in electronvolts), which is, however, a static parameter that corresponds to the given geometry and wave function and does not coincide with the dissociation energy of a given bond [21, 22]. Nevertheless, the bonding energy contributions represent useful measures of the actual strength of a chemical bond and the change in strength under different conditions (ionization, protonation, etc.). The energy contribution is usually a large negative number for neighboring atoms of a chemical bond: a more negative contribution to the total energy indicates a more stable stronger bond. For example, for the $H_2O$ molecule, the total MNDO energy (−351.42483 eV) is the sum of the monatomic (H and O) and diatomic (O—H, H—H) energy contributions as shown below:

$$\begin{aligned} -351.4249\ \text{eV} = {} & 2(-7.7169)_{\text{H}} + (-307.8287)_{\text{O}} \\ & + 2(-14.4255)_{\text{O—H}} \\ & + (+0.6886)_{\text{H—H}}\ \text{eV} \end{aligned}$$

Although bond orders and energy components are different types of quantities, there is a good qualitative correlation between them for small organic ions [21, 22]. Note that the method of energy partitioning also can be used for ions in excited (hole) states; for details, refer to refs 21 and 22.

This work is a continuation and extension of our recent work on protonated peptides [33]. By using the 6-31G* equilibrium geometries of protonated glycines and diglycines published recently by Zhang et al. [18], we calculated the 6-31G* bond orders for these species and compared them to those obtained at the MNDO level. In addition to these systems, MNDO bond orders and diatomic energy contributions are calculated and compared for $Ala_2$ and $Gly_3$ and their protonated forms. In this article, our attention is focused on a comparative investigation of bond orders and diatomic energy values. Two main questions are addressed: (1) Do bond orders and diatomic energy contributions lead to the same prediction regarding which bonds are strengthened or weakened when a peptide is protonated and (2) do MNDO and ab initio results suggest the same trends? The bond orders and diatomic energy terms of a given protonated form relative to the corresponding values for the neutral or other protonated forms are the parameters of interest. The studies do not address in detail some important questions, such as the description of H bonds, or the role of C or N terminal basic group(s) in peptide fragmentation. Related investigations are in progress in our laboratory and the results will be presented in another article.

## Results and Discussion

### *Glycine (I) and its N-Protonated (II) and O-Protonated (III) Forms*

6-31G* bond orders calculated for the neutral glycine (**I**) and its N- and O-protonated forms (**II** and **III**, respectively) at the corresponding 6-31G* optimized geometries are shown in Figure 1. For completeness, all these values (6-31G*//6-31G*) are listed in Table 1 together with MNDO bond orders and energy partitioning values obtained at both the 6-31G* (MNDO//6-31G*) and MNDO (MNDO//MNDO) equilibrium geometries. The absolute values of bond orders are close to the classically expected values of 1 and 2, for single and double bonds, respectively. Their relative changes also reflect what is expected intu-

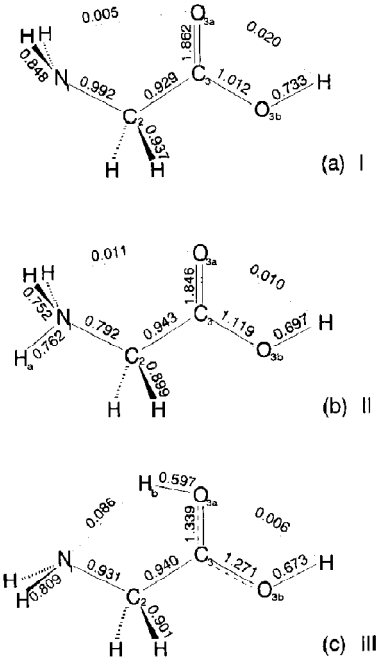


**Figure 1.** 6-31G*//6-31G* bond orders in (**a**) glycine (**I**), (**b**) N-protonated glycine (**II**), and (**c**) O-protonated glycine (**III**). (All values were obtained at the 6-31G* optimized geometries reported in ref 18.)

**Table 1.** 6-31G* and MNDO bond orders (top numbers) and MNDO diatomic energy contributions (negative values, in electronvolts) in glycine (I), $N_1$-protonated glycine (II), and $O_{3a}$-protonated glycine (III).[a]

| | I | | | II ($N_1$) | | | III ($O_{3a}$) | | |
|---|---|---|---|---|---|---|---|---|---|
| Bond | 6-31G*[b] | MNDO[c] | MNDO[d] | 6-31G*[b] | MNDO[c] | MNDO[d] | 6-31G*[b] | MNDO[c] | MNDO[d] |
| $N_1—C_2$ | 0.992 | 1.015 | 1.012 | 0.792 | 0.899 | 0.888 | 0.931 | 1.023 | 1.030 |
| | | −15.76 | −15.60 | | −13.69 | −13.40 | | −16.00 | −16.00 |
| $C_2—C_3$ | 0.929 | 0.889 | 0.881 | 0.943 | 0.892 | 0.896 | 0.940 | 0.897 | 0.864 |
| | | −14.38 | −14.11 | | −14.48 | −14.38 | | −14.27 | −13.41 |
| $C_3—O_{3a}$ | 1.862 | 1.835 | 1.816 | 1.846 | 1.827 | 1.827 | 1.339 | 1.382 | 1.321 |
| | | −26.99 | −26.32 | | −26.99 | −26.41 | | −21.47 | −20.78 |
| $C_3—O_{3b}$ | 1.012 | 1.051 | 1.042 | 1.119 | 1.123 | 1.096 | 1.271 | 1.365 | 1.347 |
| | | −17.67 | −17.53 | | −18.87 | −18.37 | | −21.35 | −20.89 |
| $O_{3b}—H$ | 0.733 | 0.934 | 0.927 | 0.697 | 0.910 | 0.907 | 0.673 | 0.888 | 0.881 |
| | | −13.96 | −14.13 | | −13.84 | −14.00 | | −13.41 | −13.57 |
| $N_1—H$ | 0.848 | 0.966 | 0.965 | 0.752 | 0.929 | 0.926 | 0.809 | 0.948 | 0.952 |
| | | −13.21 | −13.21 | | −12.74 | −12.71 | | −13.52 | −13.40 |
| $C_2—H$ | 0.937 | 0.961 | 0.959 | 0.899 | 0.960 | 0.957 | 0.901 | 0.952 | 0.948 |
| | | −12.46 | −12.37 | | −12.53 | −12.38 | | −12.39 | −12.30 |
| $N_1—H_a$ | — | — | — | 0.762 | 0.930 | 0.931 | — | — | — |
| | | | | | −12.82 | −12.76 | | | |
| $O_{3a}—H_b$ | — | — | — | — | — | — | 0.597 | 0.855 | 0.875 |
| | | | | | | | | −13.00 | −13.71 |
| $O_{3a} \cdots H$ | 0.020 | 0.006 | 0.006 | 0.010 | 0.004 | 0.004 | 0.006 | 0.007 | 0.006 |
| | | −0.24 | −0.32 | | −0.29 | −0.32 | | −0.10 | −0.25 |
| $O_{3a} \cdots H(N_1)$ | 0.005 | 0.000 | 0.000 | 0.011 | 0.001 | 0.000 | — | — | — |
| | | −0.16 | −0.17 | | −0.34 | −0.33 | | | |
| $N_1 \cdots H_b$ | — | — | — | — | — | — | 0.086 | 0.027 | 0.002 |
| | | | | | | | | −1.05 | −0.67 |

[a] The numbering of atoms is shown in Figure 1a–c.
[b] 6-31G*//6-31G* values obtained at the 6-31G* equilibrium geometries of ref 18.
[c] MNDO//6-31G* values obtained at the 6-31G* SCF equilibrium geometries of ref 18.
[d] MNDO//MNDO values obtained at the MNDO equilibrium geometries.

itively. In the N-protonated form (II), the most significant relative change is associated with the $N_1—C_2$ bond; the calculated bond order for this bond is smaller (by about 20%) than in the corresponding neutral (I), which indicates the weakening of the nitrogen–carbon bond. For the O-protonated form (III), the significant decrease in the $C_3—O_{3a}$ carbonyl bond order and increase in the $C_3—O_{3b}$ bond order lead to the suggestion that the two C—O bonds are approximately equivalent. The slight differences can be explained by the existence of a relatively strong $N_1 \cdots H_b \cdots O_{3a}$ hydrogen bond. The $H_b$ hydrogen is partially bound to the nitrogen atom; therefore, the $C_3—O_{3a}$ bond is slightly stronger than the $C_3—O_{3b}$ bond. This H bond leads also to the weakening of the $N_1—C_2$ bond although to a significantly lesser extent than in the "pure" N-protonated form. The bond orders for the H bonds are less than 10% of the bond order values for "normal" covalent single bonds.

The 6-31G* bond orders calculated for bonds involving the H atom are characteristically less than unity. This is especially true for highly polarized O—H and N—H bonds [41], the relative changes of which are also of interest and in line with classical expectations. [Note that bond orders describe the covalent character of a bond (see refs 34–36), so it is not surprising that for polar bonds their values are characteristically less than unity. This effect is even more pronounced by medium size, less balanced basis sets, for example, 3-21G and 4-31G. Recall at this point that, according to their definition, MMA bond order values are dependent on the basis set: besides well balanced basis sets, such as 6-31G** and 6-311G**, the minimal basis STO-3G has been proven to give the most reliable bond indexes (see, e.g., refs 30, 35, 36, and 41).]

Figures 2 and 3 show the MNDO//MNDO bond orders and diatomic energy terms, respectively, for species I–III. In general, there is good agreement between 6-31G* and MNDO bond orders, as well as between the relative changes in both MNDO bond orders and the diatomic energy terms. The main trends obtained by the 6-31G* basis set are "reproduced" by the semiempirical MNDO method. However, it is also clear from comparison of the data in Figures 1 and 2 that the relative strengths of H bonds in I–III cannot be predicted well by MNDO bond orders that are very

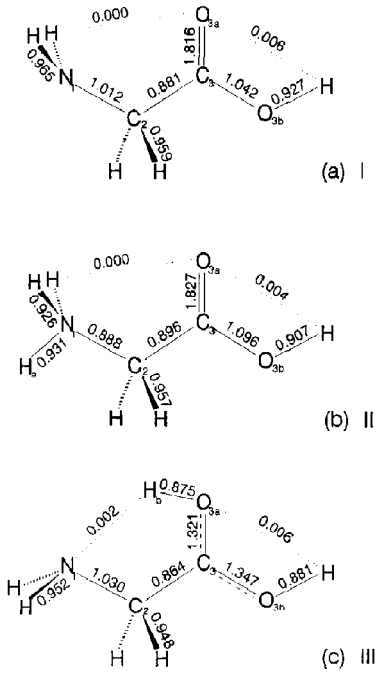


**Figure 2.** MNDO//MNDO bond orders in (a) glycine (I), (b) N-protonated glycine (II), and (c) O-protonated glycine (III). (All values were obtained at MNDO optimized geometries.)

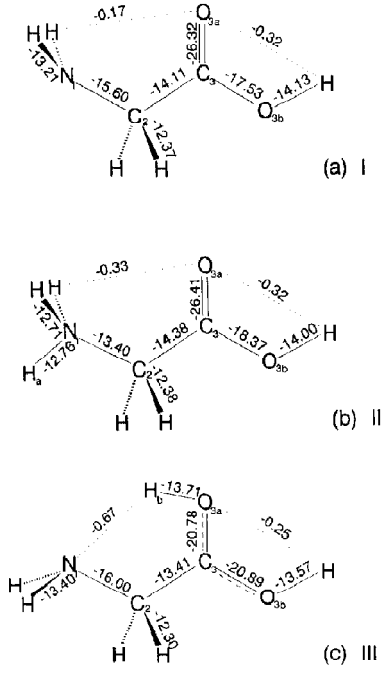


**Figure 3.** MNDO//MNDO diatomic energy contributions (electronvolts) in (a) glycine (I), (b) N-protonated glycine (II), and (c) O-protonated glycine (III). (All values were obtained at MNDO optimized geometries.)

close to zero. Fortunately, MNDO diatomic energy contributions reflect quite well the order of the H bonds; for example, the strongest H bond, $N_1 \cdots H_b—O_{3a}$, in III (by 6-31G*) has the most negative MNDO energy partitioning value (−0.67 eV). Note that the $O_{3a} \cdots H(O_{3b})$ interaction relative to the $N_1 \cdots H_b(O_{3a})$ interaction is overestimated by the MNDO energy term in III if 6-31G* bond orders are used as reference values (compare MNDO energy contributions −0.67 eV versus −0.25 eV, in Figure 3 to 6-31G* bond orders 0.086 versus 0.006, in Figure 1). As mentioned above, the corresponding MNDO bond orders are very small: 0.002 and 0.006, respectively (Figure 2). (Note that our MNDO energy partitioning contributions for H bonds are in good agreement with MNDO–PM3 values reported recently by Abliz et al. [42] for pyridinobenzanthrones and benzobenzanthranes.)

### *Diglycine (IV) and Its Protonated Forms (V–VIII)*

6-31G* and MNDO bond orders and MNDO diatomic energy contributions for diglycine (**IV**) and its protonated forms (**V–VIII**) are collected in Table 2. For simplicity, values for X—H bonds are generally omitted (X = C, N, O), and only those values that reflect (weak) H bonds in the different forms are shown. The numbering of atoms is given in Scheme II.

To discuss the chemical meaning of the numbers in Table 2 and to simplify the comparison between the ab initio and MNDO bond orders, as well as MNDO bond orders and energy partitioning values, we use a representation in which the relative changes of the above quantities [Δ (%)] are shown (e.g., see Fig. 4). The reference is always the neutral (unprotonated) peptide, and the relative changes are calculated according to the formula

$$[\text{abs}(i)^{\text{protonated}} - \text{abs}(i)^{\text{neutral}}]/\text{abs}(i)^{\text{neutral}} = \Delta\ (\%)$$

where abs($i$) indicates the absolute value of bond order or diatomic energy contribution of a given bond. Because the diatomic energy contributions are negative numbers, the difference in their absolute values will be negative according to the above definition if the bond has a lower contribution to the total energy, that is, when the bond is weakened by protonation. This way bond weakening and strengthening are indicated by negative and positive numbers, respectively, for both relative bond orders and relative diatomic energy contributions.

Figure 4a–e shows the relative changes in bond orders and MNDO diatomic energy contributions for four different protonated forms of diglycine. The changes in the bond orders and energy partitioning values are indicated from left to right in the figure for protonation at basic sites from the N terminus to the C terminus. To study the effect of different conformations, two different conformations of the N-terminal ($N_1$) protonated forms [18] are also given (**Va** and **Vb**

**Table 2.** 6-31G* and MNDO bond orders (top numbers) and diatomic energy contributions (negative numbers, in electronvolts) in diglycine (**IV**), $N_1$-protonated diglycine (**Va, Vb**), $O_{3a}$-protonated diglycine (**VI**), $N_4$-protonated diglycine (**VII**), and $O_{6a}$-protonated diglycine (**VIII**)[a]

| | IV | | | Va ($N_1$) | | | Vb ($N_1$) | | | VI ($O_{3a}$) | | | VII ($N_4$) | | | VIII ($O_{6a}$) | | |
|---|---|---|---|---|---|---|---|---|---|---|---|---|---|---|---|---|---|---|
| Bond | 6-31G*[b] | MNDO[c] | MNDO[d] | 6-31G*[b] | MNDO[c] | MNDO[d] | 6-31G*[b] | MNDO[c] | MNDO[d] | 6-31G*[b] | MNDO[c] | MNDO[d] | 6-31G*[b] | MNDO[c] | MNDO[d] | 6-31G*[b] | MNDO[c] | MNDO[d] |
| $N_1—C_2$ | 1.006 | 1.015 | 1.011 | 0.804 | 0.901 | 0.890 | 0.817 | 0.898 | 0.885 | 0.942 | 1.021 | 1.024 | 0.927 | 1.011 | 1.018 | 1.030 | 1.032 | 1.028 |
| | | −15.65 | −15.50 | | −13.55 | −13.42 | | −13.55 | −13.33 | | −15.96 | −15.79 | | −15.73 | −15.77 | | −16.20 | −15.90 |
| $C_2—C_3$ | 0.924 | 0.887 | 0.881 | 0.926 | 0.880 | 0.879 | 0.905 | 0.879 | 0.876 | 0.936 | 0.904 | 0.887 | 0.926 | 0.881 | 0.864 | 0.910 | 0.871 | 0.861 |
| | | −14.30 | −14.12 | | −14.23 | −14.14 | | −14.18 | −14.11 | | −14.31 | −13.89 | | −14.28 | −13.83 | | −14.06 | −13.78 |
| $C_3—O_{3a}$ | 1.801 | 1.835 | 1.839 | 1.731 | 1.809 | 1.823 | 1.762 | 1.839 | 1.848 | 1.252 | 1.325 | 1.289 | 2.007 | 2.109 | 2.099 | 1.781 | 1.854 | 1.892 |
| | | −27.03 | −26.67 | | −26.78 | −26.58 | | −27.00 | −26.69 | | −20.97 | −20.52 | | −29.14 | −28.60 | | −27.06 | −27.01 |
| $C_3—N_4$ | 1.012 | 1.037 | 1.003 | 1.137 | 1.120 | 1.092 | 1.104 | 1.099 | 1.072 | 1.348 | 1.444 | 1.417 | 0.712 | 0.729 | 0.704 | 0.924 | 0.974 | 0.919 |
| | | −18.08 | −17.40 | | −19.45 | −18.72 | | −18.94 | −18.61 | | −22.27 | −21.63 | | −12.04 | −11.38 | | −17.04 | −16.10 |
| $N_4—C_5$ | 0.910 | 0.956 | 0.950 | 0.859 | 0.923 | 0.914 | 0.877 | 0.931 | 0.916 | 0.815 | 0.892 | 0.879 | 0.779 | 0.900 | 0.885 | 0.912 | 0.972 | 0.984 |
| | | −16.00 | −15.97 | | −15.43 | −15.36 | | −15.48 | −15.52 | | −14.77 | −14.57 | | −13.83 | −13.37 | | −15.98 | −16.26 |
| $C_5—C_6$ | 0.941 | 0.892 | 0.884 | 0.943 | 0.898 | 0.892 | 0.946 | 0.894 | 0.891 | 0.937 | 0.890 | 0.895 | 0.952 | 0.896 | 0.899 | 0.946 | 0.906 | 0.860 |
| | | −14.30 | −14.01 | | −14.36 | −14.09 | | −14.20 | −14.01 | | −14.27 | −14.17 | | −14.52 | −14.38 | | −14.27 | −13.20 |
| $C_6—O_{6a}$ | 1.861 | 1.839 | 1.821 | 1.841 | 1.828 | 1.798 | 1.734 | 1.742 | 1.771 | 1.862 | 1.831 | 1.818 | 1.819 | 1.817 | 1.823 | 1.263 | 1.338 | 1.305 |
| | | −27.08 | −26.40 | | −27.09 | −26.26 | | −26.55 | −26.14 | | −27.08 | −26.38 | | −26.90 | −26.37 | | −21.17 | −20.60 |
| $C_5—C_{6b}$ | 1.023 | 1.053 | 1.041 | 1.070 | 1.063 | 1.076 | 1.105 | 1.133 | 1.090 | 1.080 | 1.098 | 1.081 | 1.112 | 1.121 | 1.090 | 1.291 | 1.387 | 1.363 |
| | | −17.75 | −17.56 | | −18.29 | −18.03 | | −18.79 | −18.20 | | −18.47 | −18.14 | | −18.82 | −18.26 | | −21.52 | −21.02 |
| $O_{6a} \cdots H(O_{6b})$ | 0.019 | 0.006 | 0.006 | 0.014 | 0.005 | 0.005 | 0.014 | 0.006 | 0.005 | 0.013 | 0.004 | 0.005 | 0.011 | 0.004 | 0.004 | 0.006 | 0.007 | 0.006 |
| | | −0.24 | −0.32 | | −0.28 | −0.36 | | −0.41 | −0.41 | | −0.28 | −0.33 | | −0.29 | −0.32 | | −0.13 | −0.26 |
| $O_{3a} \cdots H(N_1)$ | 0.006 | 0.000 | 0.000 | 0.060 | 0.000 | 0.001 | 0.029 | 0.000 | 0.001 | — | — | — | — | — | — | — | — | — |
| | | −0.15 | −0.16 | | −0.50 | −0.34 | | −0.33 | −0.30 | | | | | | | | | |
| $O_{6a} \cdots H(N_1)$ | 0.000 | 0.000 | 0.000 | 0.000 | 0.000 | 0.000 | 0.037 | 0.004 | 0.000 | — | — | — | — | — | — | — | — | — |
| | | −0.11 | −0.11 | | −0.26 | −0.28 | | −0.61 | −0.44 | | | | | | | | | |
| $N_1 \cdots H(O_{3a})$ | — | — | — | — | — | — | — | — | — | 0.082 | 0.026 | 0.003 | — | — | — | — | — | — |
| | | | | | | | | | | | −0.97 | −0.64 | | | | | | |
| $O_{6a} \cdots H(N_4)$ | — | — | — | — | — | — | — | — | — | — | — | — | 0.055 | 0.013 | 0.000 | — | — | — |
| | | | | | | | | | | | | | | −0.44 | −0.31 | | | |
| $N_1 \cdots H(N_4)$ | — | — | — | — | — | — | — | — | — | — | — | — | 0.064 | 0.012 | 0.002 | — | — | — |
| | | | | | | | | | | | | | | −0.63 | −0.47 | | | |
| $N_4 \cdots H(O_{6a})$ | — | — | — | — | — | — | — | — | — | — | — | — | — | — | — | 0.030 | 0.004 | 0.000 |
| | | | | | | | | | | | | | | | | | −0.76 | −0.72 |

[a] The numbering of atoms is shown in Scheme II. For simplicity, the X—H (X = C, N, and O) bond orders are omitted.
[b] 6-31G*//6-31G* values obtained at the 6-31G* equilibrium geometries of ref 18.
[c] MNDO//6-31G* values obtained at the 6-31G* equilibrium geometries of ref 18.
[d] MNDO//MNDO values obtained at the MNDO equilibrium geometries.

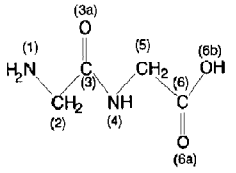


**Scheme II**

in Table 2, and Figure 4a and b; their structures are given in Scheme III).

The protonation on the terminal nitrogen ($N_1$) atom (Figure 4a and b) leads to decreasing $N_1—C_2$ bond order and a lower diatomic energy contribution to the total energy, in agreement with intuitive expectations. From these forms, the loss of $NH_3$ is, therefore, predicted. [For a recent experimental observation of $NH_3$ loss from an **a** + **1** (N-terminal protonated) ion, see ref 43.] N-terminal protonation also leads to a slight, but characteristic, strengthening of the amide bond by about 5 to 10%. This suggests that the cleavage of the amide bond could be less favorable from this form. For the other bonds, the $N_1$ protonation has no significant effect: the changes, in general, are less than 5%. It is reasonable to assume that if the chain were longer, the remote backbone bonds also would not be affected significantly. Of course, if a stable H bond can be formed, for example, between the remote amino and carboxy termini, all the chemical bonds close to the H bond will be affected. This effect is seen by the com-

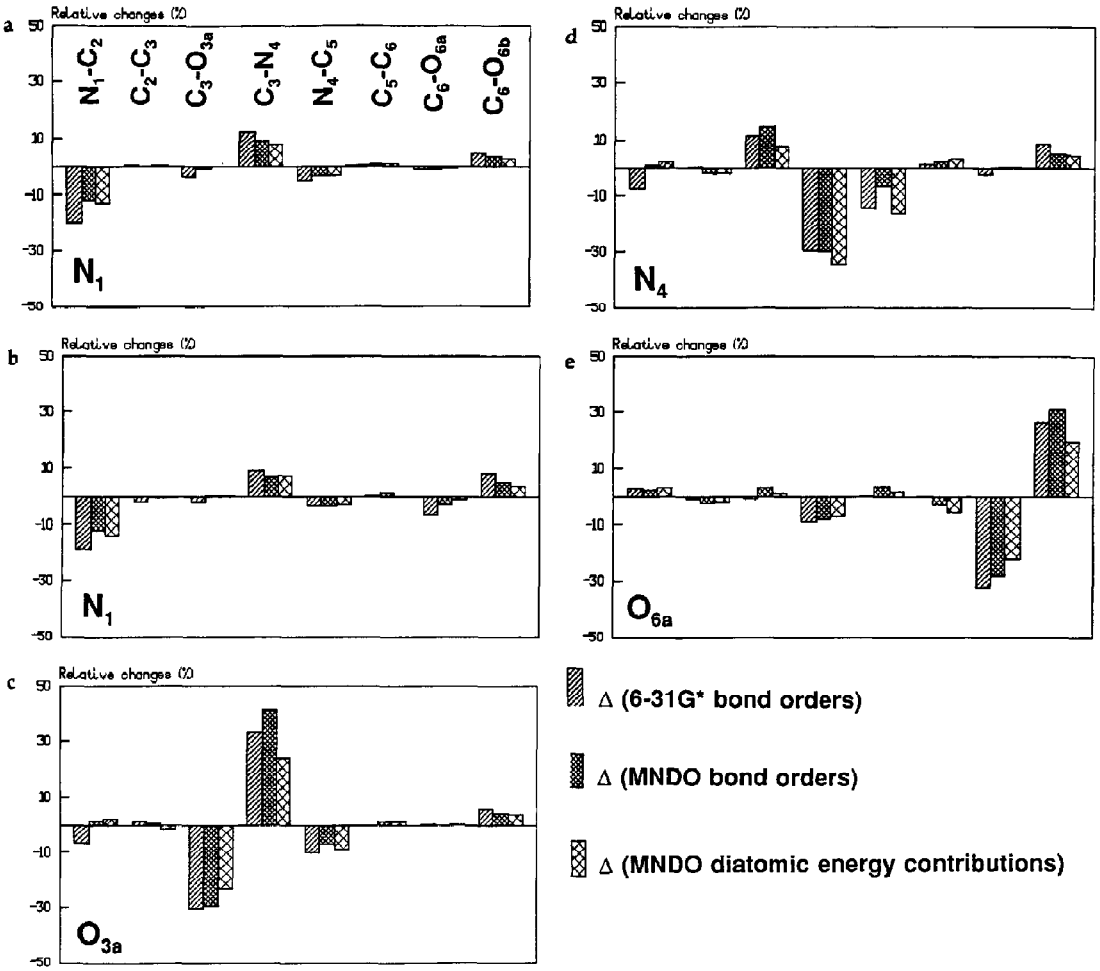


**Figure 4.** Relative changes in 6-31G*//6-31G* and MNDO//MNDO bond orders and MNDO//MNDO diatomic energy contributions in protonated diglycines. [Relative changes are referenced to the neutral, thus defined as $\Delta\% = \{abs(i)^{protonated\ form} - abs(i)^{neutral}\}/abs(i)^{neutral}$; see text for details.]

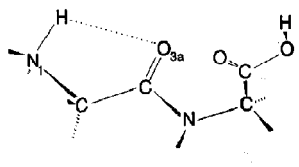

Va

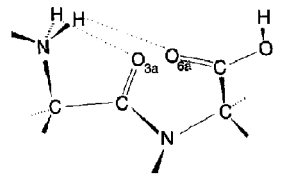

Vb

**Scheme III**

parison of Figure 4a and b. In Figure 4b, the carbonyl C=O bond is predicted to be slightly weaker by 6-31G* bond orders due to an interaction between one of the N-terminal amino hydrogens with the C-terminal carbonyl oxygen ($O_{6a}$). (In **Vb**, the distance between these atoms is 2.247 Å [18]; see Scheme III.)

The protonation on the amide oxygen ($O_{3a}$; Figure 4c) leads to a significant weakening of the $C_3{=}O_{3a}$ carbonyl bond and a significant strengthening of the amide $C_3{-}N_4$ bond. The $N_4{-}C_5$ bond becomes slightly weaker, but the other bonds are not affected. The significant stabilization of the amide bond in this $O_{3a}$-protonated form could inhibit the cleavage of this bond. This means that the formation of the **b** ions, and presumably of the **a** and **y** ions, is much less probable from this form than from the amide N-protonated form (see below).

The protonation on the amide nitrogen ($N_4$; Figure 4d) has an opposite effect, which is manifested in the significant weakening of the amide bond (by about 30%) and strengthening of the carbonyl bond (by about 10 to 15%), as we previously reported for simple model dipeptides [33]. The formation of the **b** ions by simple cleavage of the amide bond from the amide N-protonated form is presumably much more preferred than from the previously discussed N-terminal ($N_1$) and carbonyl oxygen ($O_{3a}$) protonated forms. The formation of the **a** and **y** ions can also be initiated by the simple bond cleavage of the amide bond. For example, loss of CO from the **b** ion could then form an **a** ion. Our recent ab initio calculations [33] confirm the easy loss of CO from the **b** ion. The cleavage of the amide bond is also a reasonable pathway to a **y** ion, as long as an additional H from the N-terminal portion of the molecule is transferred to the incipient **y** ion. Note that in this amide N-protonated form the $N_4{-}C_5$ bond is weaker than in any of the other protonated forms, so the direct formation of **z** ions might compete with **b** ion formation if enough energy were available.

The protonation of the terminal carboxyl oxygen ($O_{6a}$; Figure 4e) leads to weakening of the carbonyl bond and strengthening of the originally single $C_6{-}O_{6a}(H)$ bond, making these bonds about the same strength. This C-terminal protonation has a slight effect on the adjacent amide bond, making it a little bit weaker. Other bonds are only slightly affected, so the picture is similar to that obtained for the N-terminal form; remote bonds of the backbone remain practically unchanged by protonation at either terminus.

In general, there is a good correlation between the 6-31G* ab initio and MNDO bond orders, not only qualitatively, but even quantitatively. This is illustrated in Figure 5, which shows the correlation between 6-31G* and MNDO bond orders calculated for the amide bond in different protonated forms. The figure also shows that the geometry has no significant effect on the correlation: the MNDO bond orders obtained at the 6-31G* equilibrium geometries (MNDO//6-31G*) and at the MNDO geometries (MNDO//MNDO) are very similar and both agree well with 6-31G* bond orders (6-31G*//6-31G*). This means that even if the MNDO method does not provide the relative energies of different conformations with appropriate accuracy, this insufficiency is not a limitation for finding the main changes in bond orders. Nevertheless, for the description of H-bond structures one cannot rely only on MNDO geometries. A good example for this is that the above mentioned slight, but characteristic, difference between the $C_6{=}O_{6a}$ 6-31G* bond orders in the two conformers of the N-terminal protonated form (**Va** and **Vb**) is not reproduced to the same extent by the MNDO method (compare Figure 4a and b).

Another small discrepancy between the 6-31G* and MNDO bond orders is observed for the relative order of $C_2{-}C_3$ and $N_4{-}C_5$ bond orders. For instance, the MNDO method predicts the $C_2{-}C_3$ bond order (0.881) smaller in the neutral diglycine (**IV**) than that of $N_4{-}C_5$ (0.950), and this order is the reverse by the 6-31G* method (0.924 versus 0.910). This could be due to the improperly balanced character of the 6-31G* basis set, which could lead to exaggerated bond polarities, that is, smaller N—C bond orders (see above). Another recently suggested [33] possible fragmentation pathway is the charge remote cleavage of the C—C bonds of the backbone, which can lead to a **d** ion via the **a + 1** precursor and a **w** ion via an (OCNH$\cdots$**z + 1**) precursor if the charge is located, respectively, on the N or C terminal. The 6-31G* results do not exclude the possibility of the alternative mechanism [33] (via OCNH$\cdots$**z + 1**) for **w** ion formation because both the $C_2{-}C_3$ and $N_4{-}C_5$ bond orders are quite close to each other and smaller than unity (0.924 and 0.910, respectively). 6-31G SCF ab initio calculations predict about the same energy requirement for the $C_2{-}C_3$ and $N_4{-}C_5$ bond cleavages in the C-terminal protonated form (**VIII**). The

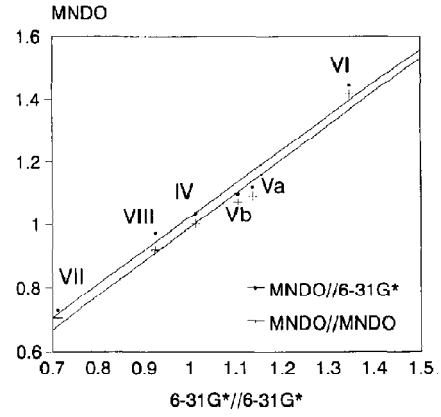


**Figure 5.** Relation between 6-31G*//6-31G* and MNDO bond orders calculated for the amide bond in neutral (**IV**) and protonated diglycines (**V–VIII**).

corresponding energy values are 78.9 and 77.2 kcal/mol for $C_2—C_3$ and for $N_4—C_5$ bond cleavages, respectively. Of course, the **w** ion could also be formed from a **z + 1** ion formed by direct N—C cleavage.

A good correlation also was found between MNDO bond orders and diatomic energy contributions, as illustrated in Figure 4. Recall that bond orders and diatomic energy components are inherently different quantities [21, 22], so the fact that they give the same trends for protonated peptides is very encouraging. We present below two other systems for the comparison of MNDO bond orders and diatomic energy contributions.

### *Dialanine and its Protonated Forms*

MNDO diatomic energy contributions and bond orders calculated for dialanine and its protonated forms are given in Table 3. Relative changes of these quantities are shown in Figure 6a–e. The numbering of atoms is shown in Scheme IV.

Characteristic similarities can be seen between the $Ala_2$ and $Gly_2$ systems (compare Figure 6 with Figure 4):

1. $N_1$-terminal amine protonation leads to the weakening of the $N_1—C_2$ bond and slight increases for the amide bond order and diatomic energy contributions.
2. The protonation on the amide oxygen ($O_{3a}$) decreases the amide carbonyl (C=O) bond strength, but increases the amide bond strength.
3. The protonation on the amide nitrogen ($N_4$) significantly decreases the amide bond strength.
4. The protonation on the terminal carbonyl oxygen ($O_{6a}$) leads to two C—O bonds with about the same strength.

**Table 3.** MNDO bond orders (top numbers) and diatomic energy contributions (negative numbers, in electronvolts) in $Ala_2$ and its protonated forms[a]

| Bond | M | $N_1$ | $O_{3a}$ | $N_4$ | $O_{6a}$ | $O_{6b}$ |
|---|---|---|---|---|---|---|
| $N_1—C_2$ | 0.993 | 0.859 | 1.041 | 1.039 | 1.004 | 1.005 |
| | −15.19 | −12.91 | −16.49 | −16.46 | −15.49 | −15.49 |
| $C_2—C_{2a}$ | 0.963 | 0.962 | 0.948 | 0.952 | 0.959 | 0.959 |
| | −14.48 | −14.51 | −14.29 | −14.36 | −14.44 | −14.43 |
| $C_2—C_3$ | 0.871 | 0.863 | 0.796 | 0.787 | 0.852 | 0.853 |
| | −14.00 | −13.90 | −12.33 | −12.60 | −13.60 | −13.62 |
| $C_3=O_{3a}$ | 1.844 | 1.865 | 1.273 | 2.122 | 1.872 | 1.835 |
| | −26.72 | −26.97 | −20.18 | −28.76 | −27.09 | −27.02 |
| $C_3—N_4$ | 1.006 | 1.069 | 1.412 | 0.669 | 0.959 | 0.981 |
| | −17.57 | −18.31 | −21.43 | −10.66 | −17.20 | −17.63 |
| $N_4—C_5$ | 0.926 | 0.913 | 0.870 | 0.873 | 0.967 | 0.970 |
| | −15.42 | −14.89 | −14.27 | −13.08 | −15.98 | −16.45 |
| $C_5—C_{5a}$ | 0.959 | 0.959 | 0.952 | 0.956 | 0.949 | 0.948 |
| | −14.43 | −14.38 | −14.33 | −14.36 | −14.26 | −14.25 |
| $C_5—C_6$ | 0.873 | 0.869 | 0.861 | 0.862 | 0.845 | 0.817 |
| | −13.93 | −13.92 | −13.80 | −13.93 | −13.16 | −12.87 |
| $C_6—O_{6a}$ | 1.866 | 1.852 | 1.883 | 1.868 | 1.345 | 2.136 |
| | −26.77 | −26.63 | −26.85 | −26.69 | −20.79 | −29.09 |
| $C_6—O_{6b}$ | 1.032 | 1.058 | 1.062 | 1.078 | 1.353 | 0.602 |
| | −17.50 | −17.81 | −17.91 | −18.10 | −20.85 | −10.66 |

[a] The numbering of atoms is given in Scheme IV. All values are calculated at the MNDO equilibrium geometries.

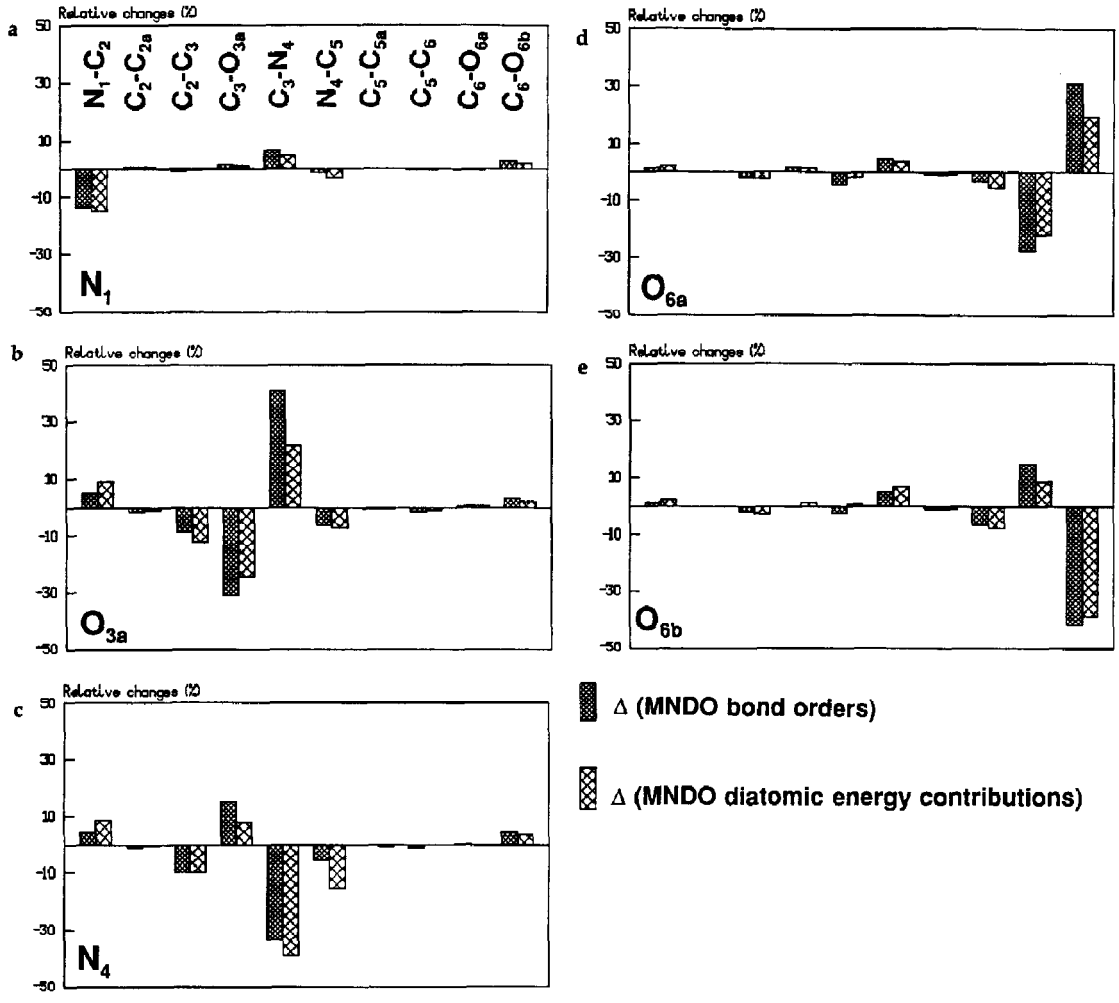


**Figure 6.** Relative changes in MNDO//MNDO bond orders and diatomic energy contributions in protonated dialanines.

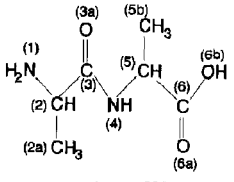


**Scheme IV**

Further comments should also be mentioned here.

5. The protonation on the OH oxygen ($O_{6b}$; Figure 6e) leads to $H_2O$ weakly bound to the rest of the backbone.
6. The $N_4$—$C_5$ bond is predicted to be slightly weakened in the $O_{3a}$- and $N_4$-protonated forms, whereas it is slightly stronger in the case of C-terminal protonations ($O_{6a}$ and $O_{6b}$).
7. The "side chain" carbon–carbon bonds ($C_2$—$C_{2a}$ and $C_5$—$C_{5a}$) remain unchanged in all protonated forms of $Ala_2$ (Figure 6), which suggests that bonds in longer side chains also are not affected by backbone protonation. (Our preliminary results on Arg–Gly, Gly–Arg, Lys–Gly, and Gly–Lys systems support this assumption.)

MNDO bond orders and diatomic energy contributions show the same trend for relative changes, although the extent of strengthening and weakening is different in some cases. For example, similarly to the diglycine system (Figure 4), the diatomic energy contributions predict lower, but still significant, relative changes for the bond weakening and bond strengthen-

ing of the carbonyl ($C_3=O_{3a}$) and amide ($C_3—N_4$) bonds, respectively, in the $O_{3a}$-protonated form (Figure 6b).

### *Triglycine and its Protonated Forms*

MNDO bond orders and diatomic energy contributions calculated for triglycine and its protonated forms are collected in Table 4. The corresponding relative changes are shown in Figure 7a–g. The numbering of atoms is shown in Scheme V.

The general picture is similar to those described above for protonated diglycines (Figure 4) and dialanines (Figure 6). However, in Figure 7, the effect of protonation is probably even much more clearly shown. Because the proton is positioned at basic sites from left to right, that is, from N-terminal protonation to C-terminal protonation, large relative values of bond strengthening or weakening follow the position of the proton, resulting in "intensity" along a diagonal in Figure 7a–g. This supports the recently drawn conclusion [33] that protonation has a local effect, that is, bonds remote from the protonation site are not affected significantly.

Another important message of Figure 7 is that the pattern of the relative changes (bond strength pattern) is very similar for the same type of protonation. For example, the general feature that illustrates strengthening and weakening is almost quantitatively the same for the two amide oxygen-protonated forms of triglycine ($O_{3a}$ and $O_{6a}$ forms; Figure 7b and d). $N_4$ and $N_7$ amide nitrogen protonations also give almost the same pattern (Figure 7c and e). Furthermore, all of the patterns for amide N-protonated forms are very similar in $Gly_2$ (Figure 4d), $Ala_2$ (Figure 6c), and $Gly_3$ (Figure 7c, and e), and this is true for the amide O-protonated patterns and N- and C-termini patterns. This is a promising result, because it suggests that the data obtained for shorter chain models can be generalized to longer oligopeptides.

However, note that the protonated peptide structure can be more complicated, that is, not only "pure" protonated forms are available, but also other structures, especially H-bond structures. These structures do not simply modify the bond strength patterns shown in Figures 4, 6, and 7, but, due to their different stability, they can also influence the energetics of fragmentation. The situation can be even more complicated if one considers that the number and the types of H bonds can presumably increase with the size of the peptide. The results for $N_1$-protonated diglycines (Figure 4a and b) and our earlier MNDO bond order calculations [33] indicate that even a particular H bond can be regarded as a local bond, that is, it influences only the nearby bonds.

**Table 4.** MNDO bond orders (top numbers) and diatomic energy contributions (negative values, in electronvolts) in $Gly_3$ and its protonated forms[a]

| Bond | M | $N_1$ | $O_{3a}$ | $N_4$ | $O_{6a}$ | $N_7$ | $O_{9a}$ | $O_{9b}$ |
|---|---|---|---|---|---|---|---|---|
| $N_1—C_2$ | 1.004 | 0.891 | 1.022 | 1.017 | 1.003 | 1.003 | 1.000 | 1.000 |
| | −15.37 | −13.44 | −15.77 | −15.71 | −15.36 | −15.36 | −15.30 | −15.29 |
| $C_2—C_3$ | 0.897 | 0.879 | 0.889 | 0.864 | 0.871 | 0.890 | 0.894 | 0.894 |
| | −14.35 | −14.13 | −13.92 | −13.85 | −14.23 | −14.18 | −14.25 | −14.26 |
| $C_3=O_{3a}$ | 1.855 | 1.826 | 1.285 | 2.095 | 1.869 | 1.832 | 1.816 | 1.819 |
| | −26.87 | −26.58 | −20.47 | −28.58 | −27.02 | −26.93 | −26.76 | −26.77 |
| $C_3—N_4$ | 0.977 | 1.089 | 1.422 | 0.710 | 0.949 | 0.972 | 1.007 | 1.005 |
| | −17.40 | −18.76 | −21.64 | −11.46 | −16.68 | −17.48 | −17.92 | −17.91 |
| $N_4—C_5$ | 0.939 | 0.907 | 0.881 | 0.886 | 0.979 | 0.982 | 0.953 | 0.953 |
| | −15.60 | −15.26 | −14.51 | −13.35 | −16.10 | −16.76 | −16.28 | −16.29 |
| $C_5—C_6$ | 0.889 | 0.883 | 0.883 | 0.884 | 0.874 | 0.832 | 0.870 | 0.872 |
| | −14.04 | −13.97 | −14.01 | −14.17 | −13.57 | −13.22 | −13.71 | −13.71 |
| $C_6=O_{6a}$ | 1.829 | 1.837 | 1.821 | 1.823 | 1.258 | 2.110 | 1.874 | 1.843 |
| | −26.69 | −26.64 | −26.59 | −26.57 | −20.15 | −28.66 | −27.02 | −26.88 |
| $C_6—N_7$ | 1.026 | 1.030 | 1.067 | 1.081 | 1.467 | 0.693 | 0.939 | 0.962 |
| | −17.94 | −18.10 | −18.36 | −18.56 | −21.96 | −11.15 | −16.55 | −16.95 |
| $N_7—C_8$ | 0.943 | 0.940 | 0.925 | 0.919 | 0.876 | 0.884 | 0.994 | 0.988 |
| | -16.01 | −16.09 | −15.55 | −15.45 | −14.49 | −13.35 | −16.54 | −16.58 |
| $C_8—C_9$ | 0.894 | 0.884 | 0.890 | 0.891 | 0.903 | 0.900 | 0.828 | 0.830 |
| | −14.09 | −13.85 | −14.08 | −14.08 | −14.26 | −14.38 | −12.68 | −13.01 |
| $C_9=O_{9a}$ | 1.831 | 1.750 | 1.804 | 1.801 | 1.824 | 1.822 | 1.312 | 2.139 |
| | −26.51 | −26.20 | −26.29 | −26.28 | −26.42 | −26.37 | −20.65 | −29.14 |
| $C_9—O_{9b}$ | 1.034 | 1.082 | 1.067 | 1.072 | 1.077 | 1.088 | 1.360 | 0.598 |
| | −17.49 | −18.06 | −17.91 | −17.96 | −18.09 | −18.24 | −20.96 | −10.67 |

[a] The numbering of atoms is given in Scheme V. All values are calculated at the MNDO equilibrium geometries.

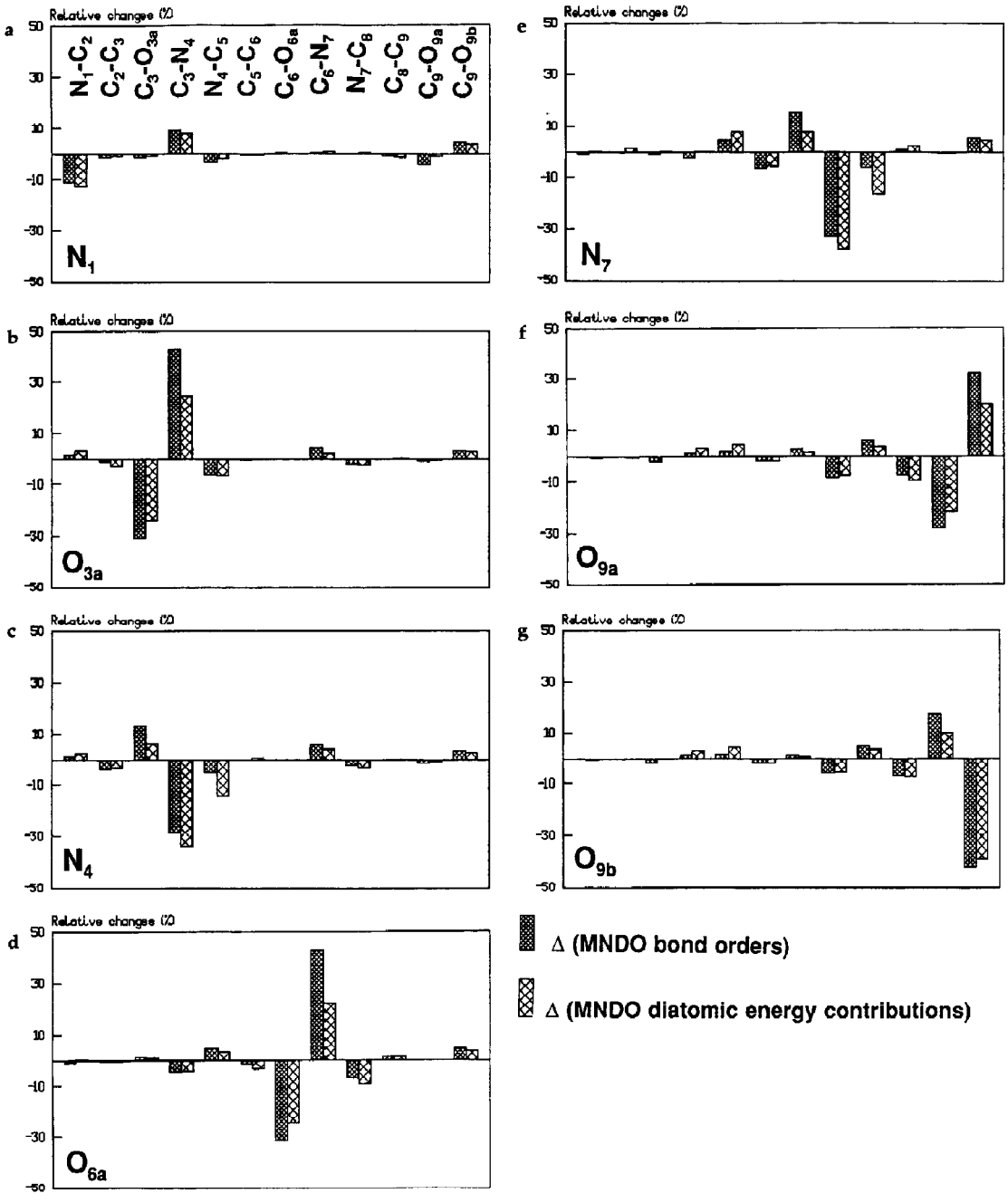


**Figure 7.** Relative changes in MNDO//MNDO bond orders and diatomic energy contributions in protonated triglycines.

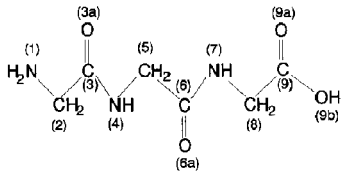


Scheme V

## Conclusions

The results presented in this article indicate that MNDO bond orders and diatomic energy contributions are both reliable quantities for the description of bond strengths in protonated peptides. We do not expect that these quantities can replace energetic treatments of mass spectral fragmentation, but we are confident that they provide a complementary approach to the interpretation and prediction of fragmentation. Similarly to recent comparative studies [29, 30], good correlations were found between ab initio 6-31G* and MNDO bond orders. Although bond orders and diatomic energy contributions are inherently different quantities, they lead to similar qualitative results, that is, they predict the same trends for relative changes in bond strengths in protonated Gly, $Gly_2$, $Gly_3$, and $Ala_2$. The similarity of the bond strength patterns for protonated $Gly_2$, $Gly_3$, and $Ala_2$ suggests that the conclusions drawn for these shorter chain models presumably can be generalized to longer oligopeptides.

The theoretical results presented here are in agreement with the proposals of other authors, such as those of Biemann and of Gaskell. Bond orders and diatomic energy partitioning contributions clearly show that different protonated forms of a peptide exhibit significant changes in bond strength in the vicinity of protonation. For example, the amide bond is strengthened or weakened if the protonation takes place on the amide oxygen and amide nitrogen, respectively. This suggests that not all protonated forms are fragmenting structures, and thermodynamically unfavorable proton transfers may be required to promote fragmentation. If the $MH^+$ has enough energy (deposited either by the ion-formation method or by the ion-activation method), the energetically less stable protonated forms can also be formed and fragment. Our recent electrospray ionization–surface-induced dissociation experiments indicate that such proton transfers occur (Jones, J. L.; Dongré, A. R.; Somogyi, Á.; Wysocki, V. H., submitted).

## Computational Details

Ab initio 6-31G* wave functions of glycine, diglycine, and their protonated isomers were determined at the equilibrium geometries given by Zhang et al. [18]. Bond orders were calculated according to the definitions in refs 34–36 by using the program package HONDO [44].

MNDO geometries were completely optimized. We used the energy partitioning scheme reported recently for the MNDO method [21, 22]. All MNDO calculations were performed by the modified PC version of the original MNDO program [19a].

## Acknowledgments

We are grateful to Kui Zhang and Dr. Carolyn Cassady (Department of Chemistry, Miami University, Oxford, Ohio) for sending us, in advance, their 6-31G* optimized geometries on glycine, diglycine, and their protonated forms (species I–VIII). The authors express their gratitude to the Hungarian Research Fund for providing computing power in the framework of grant OTKA C0020, and to the American Society for Mass Spectrometry for partial support of this project through a research award to VHW.

## References

1. Biemann, K. *Biomed. Environ. Mass Spectrom.* **1988**, *16*, 99–111.
2. Johnston, R. S.; Martin, S. A.; Biemann, K. *Int. J. Mass Spectrom. Ion Processes* **1988**, *86*, 137–154.
3. Ballard, K. D.; Gaskell, S. J. *Int. J. Mass Spectrom. Ion Processes* **1991**, *111*, 173–189.
4. Burlet, O.; Orkiszewski, R. S.; Ballard, K. D.; Gaskell, S. J. *Rapid Commun. Mass Spectrom.* **1992**, *6*, 658–662.
5. Ballard, K. D.; Gaskell, S. J. *Proceedings of the 40th ASMS Conference on Mass Spectrometry and Allied Topics*; San Francisco, 1993; Abstract 920.
6. Yeh, R.W.; Grimley, J. M.; Bursey, M. M. *Biol. Mass Spectrom.* **1991**, *20*, 443–450.
7. (a) Grese, R. P.; Cerny, R. L.; Gross, M. L. *J. Am. Chem. Soc.* **1989**, *111*, 2835–2842. (b) Leary, J. A.; Zhou, Z.; Ogden, S. A.; Williams, T. D. *J. Am. Soc. Mass Spectrom.* **1990**, *1*, 473–480. (c) Teesch, L. M.; Adams, J. *J. Am. Chem. Soc.* **1991**, *113*, 812–820.
8. Tung, X.; Boyd, R. K. *Rapid Comm. Mass Spectrom.* **1992**, *6*, 651–657.
9. (a) Mallis, L. M.; Russell, D. H. *Anal. Chem.* **1986**, *58*, 1076–1080. (b) Russell, D. H.; McGlohon, E. S.; Mallis, L. M. *Anal. Chem.* **1988**, *60*, 1818–1824.
10. (a) Watson, J. T.; Wagner, D. S.; Chang, Y.-S.; Strahler, J. R.; Hanash, S. M.; Gage, D. A. *Int. J. Mass Spectrom. Ion Processes* **1991**, *111*, 191–209. (b) Wagner, D. S.; Salari, A.; Gage, D. A.; Leykam, J.; Fetter, J.; Hollingsworth, R.; Watson, J. T. *Biol. Mass Spectrom.* **1991**, *20*, 419–425.
11. (a) Cordero, M. M.; Boyle, S. V.; Wesdemiotis, C. *Proceedings of the 40th ASMS Conference on Mass Spectrometry and Allied Topics*; Washington DC, 1992; pp 41–42. (b) Cordero, M. M.; Houser, J. J.; Wesdemiotis, C. *Anal. Chem.*, **1993**, *65*, 1594–1601.
12. Kenny, P. T. M.; Nomoto, K.; Orlando, R. *Rapid Comm. Mass Spectrom.* **1992**, *6*, 95–97.
13. Bliznyuk, A. A.; Schaefer, III, H. F.; Amster, I. J. *J. Am. Chem. Soc.* **1993**, *115*, 5149–5154.
14. (a) Smith, B. J.; Radom, L. *J. Am. Chem. Soc.* **1993**, *115*, 4885–4888. (b) Szulejko, J. E.; McMahon, T. B. *J. Am. Chem. Soc.* **1993**, *115*, 7839–7848.
15. X. Cheng, Z. Wu; Fenselau, C. *J. Am. Chem. Soc.* **1993**, *115*, 4844–4848.
16. (a) Császár, A. G. *J. Am. Chem. Soc.* **1992**, *114*, 9568–9575. (b) Perczel, A.; McAllister, M. A.; Császár, P.; Csizmadia, I. G. *J.*

*Am. Chem. Soc.* **1993**, *115*, 4849–4858. (c) Schäfer, L.; Newton, S. Q.; Cao, M.; Peeters, A.; Van Alsenoy, C.; Wolinski, K.; Momany, F. A. *J. Am. Chem. Soc.* **1993**, *115*, 272–280.
17. (a) Jensen, F. *J. Am. Chem. Soc.* **1992**, *114*, 9533–9537. (b) Bouchonnet, S.; Hoppilliard, Y. *Org. Mass Spectrom.* **1992**, *27*, 71–76.
18. Zhang, K.; Zimmerman, D. M.; Chung-Phillips, A.; Cassady, C. J. *J. Am. Chem. Soc.*, in press.
19. (a) Dewar, M. J. S.; Thiel, W. *J. Am. Chem. Soc.* **1977**, *99*, 4899–4906. (b) Stewart, J. J. P. *J. Comp. Chem.* **1989**, *9*, 209–220. (c) Dewar, M. J. S.; Zoebish, E. G.; Healy, E. F.; Stewart, J. J. P. *J. Am. Chem. Soc.* **1985**, *107*, 3902–3909.
20. Radom, L. *Org. Mass Spectrom.* **1991**, *26*, 359–373.
21. Mayer, I.; Gömöry, Á. *J. Mol. Struct. Theochem.*, in press.
22. Mayer, I.; Gömöry, Á. *Int. J. Quantum Chem. Symp.* **1993**, *27*, 599–605.
23. Somogyi, Á.; Gömöry, Á.; Vékey, K.; Tamás, J. *Org. Mass Spectrom.* **1991**, *26*, 936–938.
24. Carlsen, L.; Egsgaard, H. *J. Am. Chem. Soc.* **1988**, *110*, 6701–6705.
25. Curcuruto, O.; Traldi, P.; Cativiela, C.; Diaz de Villegas, M. D.; Garcia, J. I.; Mayoral, J. A.; Ajo, D. *J. Heterocyclic Chem.* **1990**, *27*, 1495–1499.
26. Curcuruto, O.; Favretto, D.; Traldi, P.; Ajo, D.; Cativiela, C.; Mayoral, J. A.; Lopez, M. P.; Fraile, J. M.; Garcia, J. I. *Org. Mass Spectrom.* 1991, *26*, 977–984.
27. Gömöry, Á.; Somogyi, Á.; Tamás, J.; Stájer, G.; Bernáth, G.; Komáromi, I. *Int. J. Mass Spectrom. Ion Processes* **1991**, *107*, 225–246.
28. Vékey, K.; Somogyi, Á.; Tamás, J.; Pócsfalvi, G. *Org. Mass Spectrom.* **1992**, *27*, 869–875.
29. Császár, A. G.; Somogyi, Á.; Pócsfalvi, G.; Traldi P. *Org. Mass Spectrom.* **1992**, *27*, 1349–1356.
30. Somogyi, Á.; Gömöry, Á. *Chem. Phys. Lett.* **1992**, *192*, 221–228.
31. Vékey, K.; Paizs, B.; Somogyi, Á.; Knausz, D.; Pócsfalvi, G. *Org. Mass Spectrom.*, **1993**, *28*, 1491–1497.
32. Pandolfo, L.; Paiaro, G.; Somogyi, Á.; Catinella, S.; Traldi, P. *Rapid Commun. Mass Spectrom.* **1993**, *7*, 132–137.
33. McCormack, A. L.; Somogyi, Á.; Dongré, A. R.; Wysocki, V. H. *Anal. Chem.* **1993**, *65*, 2859–2872.
34. Giambiagi, M.; de Giambiagi, M. S.; Grempel, D. R.; Heynmann, C. D. *J. Chim. Phys.* **1975**, *72*, 15–22.
35. Mayer I. *Chem. Phys. Lett.* **1983**, *97*, 270–274; **1985**, *117*, 396.
36. Mayer I. *Int. J. Quantum Chem.* **1986**, *29*, 73–84; **1986**, *29*, 477–483.
37. Reed, A. E.; Schleyer, P. v. R. *J. Am. Chem. Soc.* **1990**, *112*, 1434–1445.
38. Wiberg, K. B. *Tetrahedron* **1968**, *24*, 1083–1096.
39. Roepstorff, P.; Fohlman, J. *Biomed. Mass Spectrom.* **1984**, *11*, 601.
40. (a) Pople, J. A.; Beveridge, D. L. *Approximate Molecular Orbital Theory*; McGraw-Hill: New York; 1970; pp 67–68. (b) Fischer, H.; Kollmar, H. *Theor. Chim. Acta* **1970**, *16*, 163.
41. Villar, H. O.; Dupuis, M. *Chem. Phys. Lett.* **1987**, *142*, 59–66.
42. Abliz, Z.; Aoki, J.; Ueda, T.; Kan, T.; Takekawa, M.; Iwashima, S. *Org. Mass Spectrom.* **1993**, *28*, 607–614.
43. Thornburg, K.R.; Schey, K.L.; Knapp, D.R. *J. Am. Soc. Mass Spectrom.* **1993**, *4*, 424–427.
44. Dupuis, M.; Farazdel, A. Program HONDO-8, IBM Corporation Center for Scientific Engineering Computations (Department 48B/428 Neighborhood Road, Kingston, NY 12401).